Mimicking Human Push-Recovery Strategy based on Five-Mass with Angular Momentum Model

Ren C.Luo, *Fellow, IEEE,* and Wen C.Hung
Electrical Engineering Department
National Taiwan University
Taipei, Taiwan
Telephone:(886)2-3366-9822
Email: renluo@ntu.edu.tw

Raja Chatila, *Fellow, IEEE*
Institut des Systèmes Intelligents et de Robotique
Université Pierre et Marie Curie
Paris, France

***Abstract*—As humanoid robots start entering to the human beings environments, the collision between the robot and other objects is inevitable. To solve this problem, we propose the human mimicking push-recovery strategy. With the arm mechanism, the humanoid robot utilizes human-like strategies to deal with the unexpected collision. We analyse the human push-recovery movement to the external force. Thus we can design the trajectory generator to mimic human beings reactions. To reduce the modelling error and improve zmp stability, we utilizes the five-mass with angular momentum model as humanoid robot model. We design the safe bound examination and the Center of Mass (COM) state estimator to judge the collision stage. The safe bound examination is used to guarantee the walking stability. Moreover, the COM state estimator is used to determine whether the pushing is over or not. The push-recovery control system is implemented on the humanoid robot developed in our NTU-iCeiRA lab. The purpose of this paper aims to integrate different push-recovery strategies while encountering different collision conditions based on the five-mass with angular momentum model.**

I. Introduction

The bipedal and humanoid robots have higher elasticity to move in the complexity environment and execute specific tasks than other kinds of robot. In the field of humanoid and biped robots, Zero Moment Point (ZMP) [1] criterion is the most commonly used criterion to determine the walking stability. ZMP criterion implies if Center of Pressure (COP) always lies inside the convex hull of support feet the humanoid is stable. Kajita et al. [2] proposed preview control which optimize the trajectory of COM and generate the walking pattern with reference ZMP trajectory. Shimmyo et al. [3] improved the preview control to more accurate result by three mass model.

As robots begin to walk away from laboratory, start entering to the general environments. Robot is inevitable to bump into other things or human beings. When these unpredictable collisions occur, robot having strategy to avoid falling down and maintain balance becomes very important. Unlike wheel robots and multi-legged robots having more stable mechanism, humanoid and biped robot only can use legs and arms to maintain its balance. So the push-recovery problem is an indispensable issue to the humanoid robots. To compensate the external perturbations Wieber et al. [4] proposed the on-line walking gait generation with Linear Model Predictive Control (LMPC). Pratt et al. [5] proposed the capture point theory to calculate the instantaneous capture point and the capture region when the large external force occurs. Kobayashi et al. [6] proposed the optimal arm-swing strategy for humanoid walking control. Albertus et al. [7] proposed a push recovery controller to process the instantaneous push and hard push. we have proposed the planar push-recovery strategy on our lab's bipedal robot [8], which used the angular momentum based on preview control.

The purpose of this paper aims to integrate different strategies while encountering different collision conditions. And figure out the coordination of the body trajectory and compensate the COM offset, affected by the unknown external force. We analyse the human push-recovery reaction when facing the external push. We classify the push direction into right-front, left-front, right-back and left-back. And we divide the

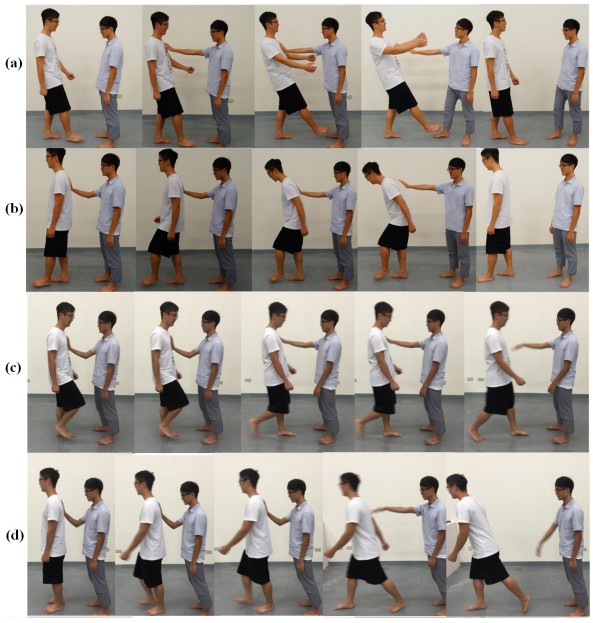

Fig. 1. Pushing test on human beings **(a)** The small push from the front. **(b)** The small push from the back. **(c)**The large push from the front**(d)**The large push from the back .

978-1-5090-3474-1/16/$31.00 ©2016 IEEE

magnitude of the push force into soft push and hard push. The definition of the hard push is that the momentum caused by push can not be compensated by the swinging arms, legs and trunk. The pushing test on the human beings is shown in Fig. 1, if the soft push is from the front the human being will swing leg and arms forward. If the soft push is from the back the human being will rotate the trunk forward and swing arms backward. If the hard push is from the front the human being will step backward. If the hard is from the back the human being will step forward to maintain it's balance.

This paper is organized as follows: in Section II, we implemented the trajectory generator based on the five-mass with angular momentum model. In Section III, we proposed the timetable of the push-recovery reaction. In Section IV, we illustrated the perturbation detection, torque distribution, motion trajectory design, definition of the safe region boundary and balance controller. In Section V, the new humanoid robot developed in our lab is introduced. In Section VI, the analysis of the experimental results is presented. Finally, the conclusions and the future work are proposed in Section VII.

II. WALKING PATTERN GENERATOR BASED ON PROPOSED MODEL

In this section we propose a precise model based on a five-mass and angular momentum model to realize humanoid robot walking pattern generator. The combination of previous three-mass model [9] and extra two mass bulks on each arm is expressed as a new ZMP description of a new system. In early research, Tomoya Sato et al. [9] [10] reduced modeling errors by a precise model expressing the whole system. To handle the compensation of the coupling effect and divide the motion into sagittal and frontal plane, we adopt a dynamic controller [11]. So, we can simplify and model a multi-mass model into a five-mass model, and observe the ZMP description in sagittal and frontal plane respectively.

A. Five-mass with angular momentum model

In this paper, we show the ZMP description in sagittal plane, which is similar for frontal not shown here. First, we simplify the entire robot shown in Fig. 2, which is composed of five mass bulks for left and right arm, M_a, left and right leg, M_1, and body, M_b. We respectively, define

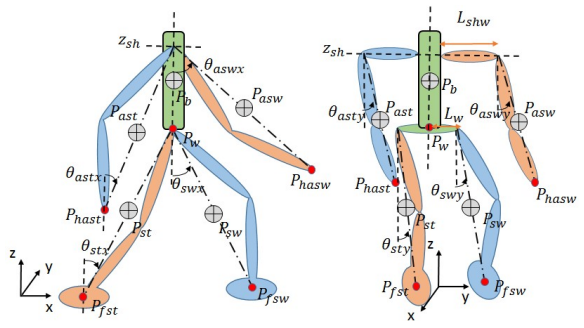

Fig. 2. Sagittal (left) and Frontal (right) plane of proposed method.

$p_w \equiv \begin{bmatrix} x_w & y_w & z_w \end{bmatrix} \in \Re^{1\times 3}$, $p_b \equiv \begin{bmatrix} x_b & y_b & z_b \end{bmatrix} \in \Re^{1\times 3}$,$p_{st} \equiv \begin{bmatrix} x_{st} & y_{st} & z_{st} \end{bmatrix} \in \Re^{1\times 3}$ and $p_{sw} \equiv \begin{bmatrix} x_{sw} & y_{sw} & z_{sw} \end{bmatrix} \in \Re^{1\times 3}$as the position of center of mass (COM), body, stance leg and swing leg.L_{lx} and L_{bx} denote the length of auxiliary line of legs, the dotted line, and the distance betweenp_w and p_b along x-coordinate, respectively. To evaluate the influence of two arm mass bulks, we further introduce other parameters into conventional three-mass model. $p_{ast} \equiv \begin{bmatrix} x_{ast} & y_{ast} & z_{ast} \end{bmatrix} \in \Re^{1\times 3}$ and $p_{asw} \equiv \begin{bmatrix} x_{asw} & y_{asw} & z_{asw} \end{bmatrix} \in \Re^{1\times 3}$ are respectively defined as the position of backward arm swinging and forward arm swinging. L_{ax} is the length of auxiliary line of arms in. By geometric relationship as the robot is walking, θ_{stx}, θ_{swx}, θ_{astx} and θ_{aswx} are respectively, angle of the stance leg, swing leg, backward arm swinging and forward arm swinging. Here, counterclockwise is defined as the positive direction in both sagittal and frontal plane of ZMP. The proposed ZMP description is shown as:

$$\begin{aligned} & I_{lx}(\ddot{\theta}_{st}+\ddot{\theta}_{sw})+I_{ax}(\ddot{\theta}_{ast}+\ddot{\theta}_{asw}) \\ & =M_l g(x_{st}-x_{zmp})+M_l g(x_{sw}-x_{zmp}) \\ & +M_a g(x_{ast}-x_{zmp})+M_a g(x_{asw}-x_{zmp}) \\ & +M_b g(x_b-x_{zmp})-M_l \ddot{x}_{st} z_{st}-M_l \ddot{x}_{sw} z_{sw} \\ & -M_b \ddot{x}_b z_b-M_a \ddot{x}_{ast} z_{ast}-M_a \ddot{x}_{asw} z_{asw}. \end{aligned} \tag{1}$$

where I_{lx} and I_{ax} are rotational inertia through taking the center of leg and arm as a pivot in sagittal plane, respectively. Here, we assign $\ddot{\theta}_b = 0$ for a normal body motion as walking, so we don't show angular momentum of body. I_{lx} and I_{ax} are respectively, defined as $\frac{1}{12}M_l L_{lx}^2$ and $\frac{1}{12}M_a L_{ax}^2$. Through the geometric relationships in Fig. 3., θ_x can be expressed in sagittal plane as following.

$$\begin{aligned} \cos\theta_{stx} &= \frac{z_w}{L_{lx}}, \quad \sin\theta_{stx} = \frac{z_w - x_{ft}}{L_{lx}} \\ \cos\theta_{swx} &= \frac{2(z_w - z_{sw})}{L_{lx}}, \quad \sin\theta_{swx} = \frac{z_w - x_{fw}}{L_{lx}} \end{aligned} \tag{2}$$

where we assume the height of waist, z_w, and center of the swing leg, z_{sw}, are constant.x_{fst} and x_{fsw} denote respectively, the position of the stance leg and the swing leg, in the x-coordinate. Moreover, θ_{astx} and θ_{aswx} can be derived by the same process in (2). Then, we further take second derivative of $\tan\theta_x$ and attain angular acceleration $\ddot{\theta}_{st}$, $\ddot{\theta}_{sw}$, $\ddot{\theta}_{ast}$ and $\ddot{\theta}_{asw}$. Furthermore, we can obtain $\ddot{x}_{st}$, $\ddot{x}_{sw}$, $\ddot{x}_{ast}$, $\ddot{x}_{asw}$ and $\ddot{x}_b$ in terms of $\ddot{x}_w$ from relationship between the velocity of waist and that of center of each mass points.

$$\begin{aligned} \ddot{x}_b &= \ddot{x}_w, \quad \ddot{x}_{st} = \frac{1}{2}\ddot{x}_w, \quad \ddot{x}_{sw} = \frac{1}{2}(\ddot{x}_w + \ddot{x}_{fw}) \\ \ddot{x}_{ast} &= \frac{1}{2}(\ddot{x}_w + \ddot{x}_{east}), \quad \ddot{x}_{asw} = \frac{1}{2}(\ddot{x}_w + \ddot{x}_{easw}) \end{aligned} \tag{3}$$

Through substituting $\ddot{\theta}_{st}$, $\ddot{\theta}_{sw}$, $\ddot{\theta}_{ast}$, $\ddot{\theta}_{asw}$, and (3) into (1), we finally can earn a rough equation for five-mass and angular momentum model as

$$
\begin{aligned}
x_{zmp} =& \frac{M-M_l-M_a}{M}x_w - H_x\ddot{x}_w + I_x\ddot{x}_{fw} - J_x\ddot{x}_{hast} \\
& - K_x\ddot{x}_{easw} + \frac{M_l}{2M}x_{fw} + \frac{M_l}{2M}x_{ft} + \frac{M_a}{2M}x_{east} \\
& + \frac{M_a}{2M}x_{easw} + V_x
\end{aligned} \tag{4}
$$

where H_x, I_x, J_x and K_x are in terms of constant, and have been known in terms of parameters, such as z_w, z_{sw}, z_{ast} and L_{bx}. However, in fact, the V_x is derived as a non-linear term, and shown as follow:

$$
\begin{aligned}
V_x =& \frac{1}{6}M_l\frac{z_w(x_w-x_{ft})}{L_{ix}^4}\dot{x}_w^2 \\
& + \frac{1}{6}M_l\frac{2(z_w-z_{sw})(x_w-x_{fw})}{L_{ix}^4}(\dot{x}_w-\dot{x}_{fw})^2 \\
& + \frac{1}{6}M_a\frac{2(z_{sh}-z_{ast})(x_w-x_{east})}{L_{ax}^4}(\dot{x}_w-\dot{x}_{east})^2 \\
& + \frac{1}{6}M_a\frac{2(z_{sh}-z_{asw})(x_w-x_{easw})}{L_{ax}^4}(\dot{x}_w-\dot{x}_{easw})^2
\end{aligned} \tag{5}
$$

So, we call (4) as a pseudo solution. Furthermore, we would need another equation to help us to deal with this non-linear term.

B. Law of Conservation of Angular Momentum for Dynamics of ZMP description

In last subsection, we obtain a rough solution for proposed method because of the non-linear term, V_x. In this subsection, we use law of angular momentum to eliminate the non-linear term in (4).

According to Fig. 2, in the sagittal plane, law of conservation of angular momentum can be expressed as

$$
\begin{aligned}
& (I_{bx}+M_bL_{bx}^2)d\vec{w}_{bx} + (I_{lx}+\frac{M_lL_{lx}^2}{4})(d\vec{w}_{stx}+d\vec{w}_{swx}) \\
& +(I_{ax}+\frac{M_aL_{ax}^2}{4})(d\vec{w}_{astx}+d\vec{w}_{aswx}) \\
& =\vec{R}_{fstx}\times\vec{F}_x + M_b\vec{R}_{bx}\times(\vec{g}+\ddot{\vec{x}}_w)dt \\
& +\frac{1}{2}M_l\vec{R}_{swx}\times(\vec{g}+\ddot{\vec{x}}_{sw})dt + \frac{1}{2}M_l\vec{R}_{stx}\times(\vec{g}+\ddot{\vec{x}}_{st})dt \\
& +\frac{1}{2}M_a\vec{R}_{astx}\times(\vec{g}+\ddot{\vec{x}}_{ast})dt + \frac{1}{2}M_a\vec{R}_{aswx}\times(\vec{g}+\ddot{\vec{x}}_{asw})dt
\end{aligned} \tag{6}
$$

where $\vec{w}_{bx}$, $\vec{w}_{stx}$, $\vec{w}_{swx}$, $\vec{w}_{astx}$ and $\vec{w}_{aswx}$ vector of differential of θ_{bx}, θ_{stx}, θ_{swx}, θ_{astx} and θ_{aswx}, respectively. $\vec{R}_{bx}$, $\vec{R}_{stx}$, $\vec{R}_{swx}$, $\vec{R}_{astx}$ and $\vec{R}_{aswx}$ position vector from waist to masses of body, stance leg, swing leg, backward arm swinging and forward arm swinging, respectively. F_x is defined as the value of ground reaction force which is perpendicular to the stance leg in sagittal plane. F_x is derived from Newton's law:

$$
\begin{aligned}
& F_k\sin\theta_{stx} - F_x\cos\theta_{stx} \\
& \qquad = M_b\ddot{x}_b + M_l(\ddot{x}_{st}+\ddot{x}_{sw}) + M_a(\ddot{x}_{ast}+\ddot{x}_{asw}) \\
& F_k\cos\theta_{stx} + F_k\sin\theta_{stx} - Mg \\
& \qquad = M_b\ddot{x}_b + M_l(\ddot{z}_{st}+\ddot{z}_{sw}) + M_a(\ddot{z}_{ast}+\ddot{z}_{asw})
\end{aligned} \tag{7}
$$

where F_k is defined as the linear actuation force from the ground on the leg in sagittal plane. Because of presumption before, $\ddot{z}_b$, $\ddot{z}_{st}$, $\ddot{z}_{sw}$, $\ddot{z}_{ast}$ and $\ddot{z}_{asw}$ are equivalent to zero. Then, we substitute $\ddot{\theta}_{st}$, $\ddot{\theta}_{sw}$, $\ddot{\theta}_{ast}$ and $\ddot{\theta}_{asw}$, and $\ddot{x}_{st}$, $\ddot{x}_{sw}$, $\ddot{x}_{ast}$, $\ddot{x}_{asw}$ and $\ddot{x}_b$, and F_x into (6). Therefore (6) can be rewritten as a similar form as (4), and the form, also consisting of a non-linear time, V_x', is shown as:

$$
\begin{aligned}
H_x'\ddot{x}_w =& (M-M_l-M_a)gx_w + I_x'\ddot{x}_{fsw} + J_x'\ddot{x}_{hast} \\
& + K_x'\ddot{x}_{easw} - (M-\frac{1}{2}M_l)gx_{ft} + \frac{1}{2}M_lgx_{fw} \\
& + \frac{1}{2}M_agx_{east} + \frac{1}{2}M_agx_{easw} + V_x'
\end{aligned} \tag{8}
$$

where

$$V_x' = 4V_xMg$$

Here, we noticeV_x' is $4Mg$ times of V_x. It means that V_x in (4) can be replaced by (8) divided by $4Mg$. Finally, the five-mass with angular momentum model can be derived.

C. Compensation from Swinging Arm and Leg motion

We have combined the arm motion into the proposed model method in last subsections. But, we didn't consider the angular momentum generated from legs and arms in walking motion. Here, we show a simple idea for balance of moment of inertia in z axis.

We express the conservation of moment of inertia in z axis as torque form like (6) does,

$$
\begin{aligned}
\tau_L &= (\vec{R}_{stx}\times\vec{F}_{stx} + \vec{R}_{swx}\times\vec{F}_{swx} + \vec{R}_{fstx}\times\vec{F}_x)\cdot\hat{k} \\
\tau_A &= (\vec{R}_{astx}\times\vec{F}_{astx} + \vec{R}_{aswx}\times\vec{F}_{aswx})\cdot\hat{k}
\end{aligned} \tag{9}
$$

where

$$
\begin{aligned}
\vec{F}_{stx} &= m_l\ddot{x}_{st}, \vec{F}_{swx} = m_l\ddot{x}_{sw} \\
\vec{F}_{astx} &= m_a\ddot{x}_{ast}, \vec{F}_{aswx} = m_a\ddot{x}_{asw}
\end{aligned}
$$

where, τ_L and τ_A respectively, denote the the torque caused by legs rotation and arm rotation, in z axis. Here, the moment generated by the legs in direction $\hat{i}$ and $\hat{j}$ are not shown because they are negligible comparing to the moment in $\hat{k}$ direction.

III. PUSH-RECOVERY TIMETABLE

The procedure of the external push counteraction in sagittal plane is shown in Fig. 3. The time external push occurs is called T_1. The stage after T_1 is defined as collision stage. In this stage the designed human-like reaction trajectory removes the effect of the push and decelerates to stop. The time swinging arms, swinging leg and rotating trunk moves back to the original trajectory is called T_2. After T_2 the last part of the counteraction motion including holding time and reverse time is called reversing stage. The holding stage is to guarantee the recovery motion is completed. The time that the swing leg steps on its reference footprint is called T_3. The procedure in lateral plane is the same with the sagittal plane.

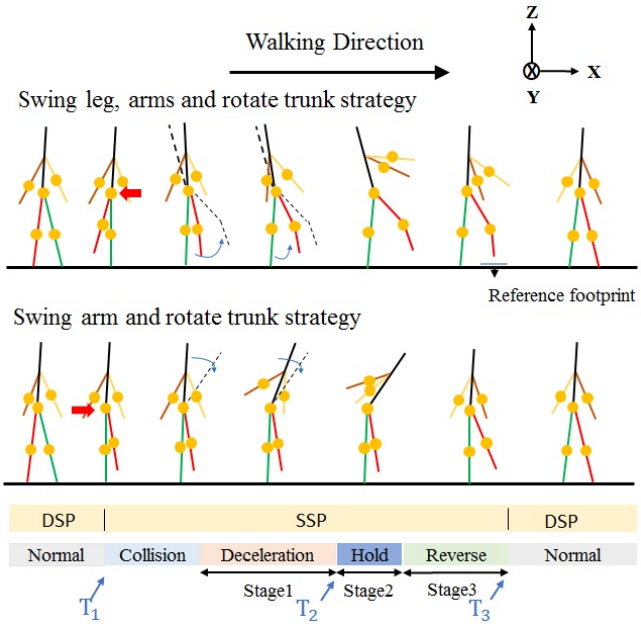

Fig. 3. Time table of the reaction when the external push occurs.

IV. PUSH-RECOVERY STRATEGY GENERATOR

A. Perturbation detection

The orbital energy [12] criterion is used to determine the magnitude when the external push. The orbital energy can be implied as follow:

$$E(t) = \frac{1}{2}\dot{r}(t)^2 - \frac{1}{2}\omega^2 r(t)^2 \tag{10}$$

Here, $r(t)$and $\dot{r}(t)$ is the COM position and the linear velocity of the COM which both can obtain by IMU sensor. $\omega = \sqrt{\frac{Z_o}{g}}$, Z_o is the constant COM height. Theoretically, during the walking time period the orbital energy will remains constant. But the complexity of the mechanism and the imprecise of the sensors the orbital energy may not maintain constant. Consequently the energy threshold is designed to judge whether the externa push still acts on humanoid robot or not.

$$|E - E_d| > \Delta E \tag{11}$$

Here, E_d denotes the regular walking orbital energy. ΔE is the threshold of the tolerable energy error.

B. Torque distribution

In this paper, we try to propose a human-like reaction strategy to maintain balance while external push occurs. To adapt to different magnitude push, an angle optimization method is used to determine the distribution of torque. The reaction rotational system is derived as

$$\phi_{k+1} = A\phi_k + Bu_k \tag{12}$$

where

$$\varphi_{k+1} = \begin{bmatrix} \theta_l & \dot{\theta}_l & \theta_t & \dot{\theta}_t & \theta_a & \dot{\theta}_a \end{bmatrix}^T$$

$$u_k = \begin{bmatrix} \tau_l & \tau_t & \tau_a \end{bmatrix}^T$$

And,

$$A = \begin{bmatrix} 1 & T & 0 & 0 & 0 & 0 \\ 0 & 1 & 0 & 0 & 0 & 0 \\ 0 & 0 & 1 & T & 0 & 0 \\ 0 & 0 & 0 & 1 & 0 & 0 \\ 0 & 0 & 0 & 0 & 1 & T \\ 0 & 0 & 0 & 0 & 0 & 1 \end{bmatrix}, B = \begin{bmatrix} \frac{T^2}{2I_l} & 0 & 0 \\ \frac{T}{I_l} & 0 & 0 \\ 0 & \frac{T^2}{2I_t} & 0 \\ 0 & \frac{T}{I_t} & 0 \\ 0 & 0 & \frac{T^2}{2I_a} \\ 0 & 0 & \frac{T}{2I_a} \end{bmatrix}$$

Here, I_l ,I_a and I_t is the momentum of the inertia of the swing leg, swing arm and trunk. T is the sampling time. θ_l, θ_a and θ_t are the angle of the swing leg, swing arm and rotate trunk. τ_l, τ_a and τ_t are the correspondence torque from swing leg, swing arm and rotate trunk. The performance index is derived as

$$P_{k+1} = \frac{1}{2}(X_{k+1}^T Q X_{k+1} + u_k^T R u_k) \tag{13}$$

Here, Q and R restrict the corresponding factors X. To avoid body collision the mechanism constraints is considered. The summary of torque is under the precondition $\tau = \tau_l + \tau_t + \tau_a$.

C. Stability balance controller

In general the purpose of feedback controller is to reduce the tracking error and regulate the operating point automatically. In our previous work, we applied the joint controller with feedback control which enable the manipulation of COM trajectory. The control law is shown as follow:

$$\ddot{P}_{com}^{des} = \ddot{P}_{com}^{ref} + K_d(\dot{P}_{com}^{des} - \dot{P}_{com}^{ref}) + K_p(P_{com}^{des} - P_{com}^{ref}) \tag{14}$$

Here,P_{com}^{res} and $\dot{P}_{com}^{res}$ denotes the COM state (position and velocity) which is calculated by Kalman filter. $\ddot{P}_{com}^{res}$, $\dot{P}_{com}^{res}$ and P_{com}^{res} the reference COM position, velocity and acceleration which is optimized by the preview control. K_d and K_p are parameters to deal with the corresponding tracking error. $\ddot{P}_{com}^{des}$ denotes the desired COM acceleration which is used in feedback control. The translation from the joint of support leg in single support phase (SSP) or the joint of the rear support leg in double support phase (DSP) to the COM motion can be implemented as $\dot{P}_{com} = J_c\dot{q}$, where $\ddot{P}_{com}^{des}$ is the jacobian matrix relative to the internal joints and $\dot{q}$ denotes the internal joint velocity. Hence the COM acceleration can be expressed as

$$\ddot{P}_{com}^{des} = J_c\ddot{q}_{ank}^{des} + J_c\dot{q} \tag{15}$$

$\ddot{q}_{ank}^{des}$ is the desired acceleration of the ankle joint of the swing leg. Due to the serial connection design mechanism, the acceleration of the ankle joint is expressed as

$$\ddot{q}_{ank}^{des} = M^{-1}(J^T F + \tau - N) \tag{16}$$

Here, J is the jocobian matrix correlation between the internal joints and front support leg. F is the ground reaction

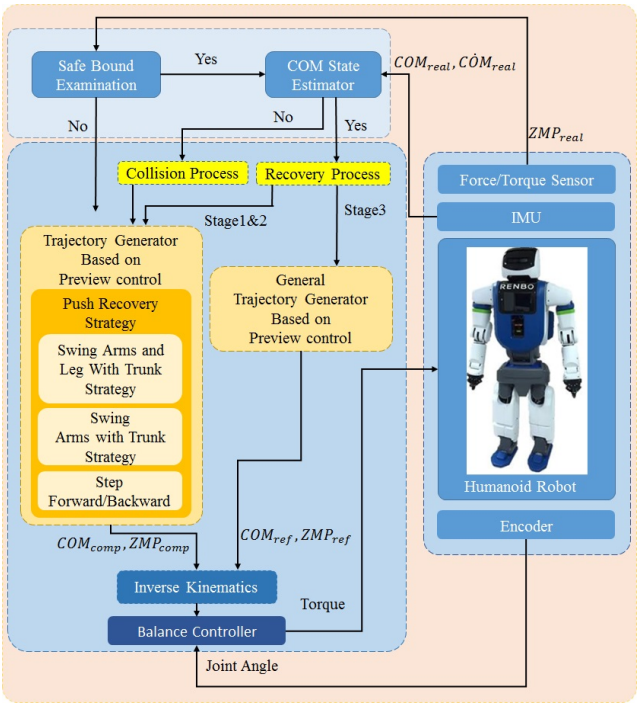

Fig. 4. Architecture of the overall control system with the push-recovery strategy.

force (GRF). M and N are the matrices of mass and nonlinear force. By solving the (22) (23)(24), the torque applying for the feedback force controller is derived as

$$\tau = MJ_c^{-1}[\ddot{P}_{com}^{ref} + K_d(\dot{P}_{com}^{res} - \dot{P}_{com}^{ref}) + K_p(P_{com}^{res} - P_{com}^{ref}) - \dot{J}_c\dot{q}] - J^T F + N \quad (17)$$

V. DEVELOPMENT OF NEW HUMANOID ROBOT

We have developed a bipedal robot with 14 Degrees Of Freedom (DOF) to mimic human beings walking action and mechanisms. But without arms and torso bipedal robot cannot mimic whole human beings motion accurately. So we develop a new humanoid robot named RENBO. Its height is 1650 mm with 75 kg weight (include the battery and the industrial computer). Each leg weights 21 kg and the momentum of the inertia is 3.56 kgm^2. Each arm weights 6 kg and the momentum of the inertia is 1.3 kgm^2. The trunk weights 21 kg and the momentum of the inertia is 3 kgm^2. All the momentum of the inertia can be used to generate the angular momentum to maintain the balance while walking. RENBO has 33 DOFs. 1 DOF for Laser Range Finder (LRF) on abdomen, 6 DOFs on each leg, 6 DOFs on each arm, 2DOFs on head, 1 DOFs on waist , 3 DOFs on trunk and two grippers.

VI. EXPERIMENTAL DATA COMMENTARY

The entire control system architecture of human mimicking push-recovery strategy is shown in Fig. 4. The general trajectory walking pattern generator is based on ZMP preview control and five-mass with angular momentum Model. The trajectory generator can generate the optimal COM trajectory by desired footprint. Besides the trajectory generator can guarantee the COP stay inside the convex hull of support feet. The force/torque sensor is installed on each sole so as to obtain the actual ZMP. Then the actual ZMP can be used to determine the safe bound examination. When the collision occurs the ZMP will be shifted. If the ZMP is not in the inner safe bound, the trajectory generator will generate the recovery strategy.

The COM state estimator classified the push-recovery action into two process. One is collision process and the other is recovery process. The recovery process can also be split into deceleration stage, hold stage and reverse stage. By different stage the trajectory generator can produce different compensate trajectory. By solving the inverse kinematics between the desired footprint and COM position, each axis joint angle can be calculated. A balance control is applied for improving the robustness while the external push occurs.

The experiments of push recovery strategy is conducted on a serial linked humanoid robot. In the first experiment, the humanoid robot is pushed from the left-front. As shown in Figure 5, the trunk, swing-leg, and swing-arms work together to maintain the stability of the walking robot. The swing leg, arms and rotate trunk strategy is applied to eliminate the ZMP sifting both in lateral and sagittal plane. In the second experiment, the humanoid robot is pushed from the right-back as shown in Figure 5. The strategy for push from left-back situation is the same as the push from right-back situation so we just analyze the situation of the push from right-back. We applied the swing arms and rotate trunk strategy in both sagittal and lateral direction. The swing, arms and rotate trunk strategy is applied to eliminate the ZMP sifting in both sagittal direction and lateral direction. The ZMP trajectory of first

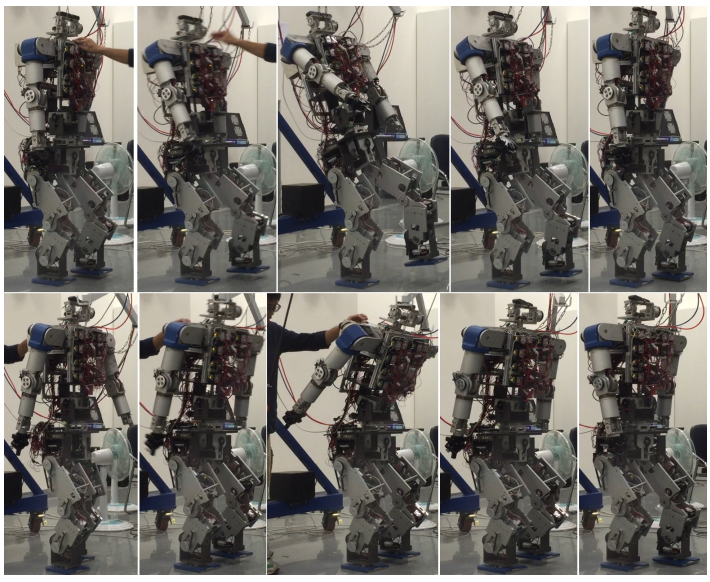

Fig. 5. First column : Snapshots of four-step walking with push from the left-front of humanoid robot. Second column: Snapshots of four-step walking with push from the right-back of humanoid robot.

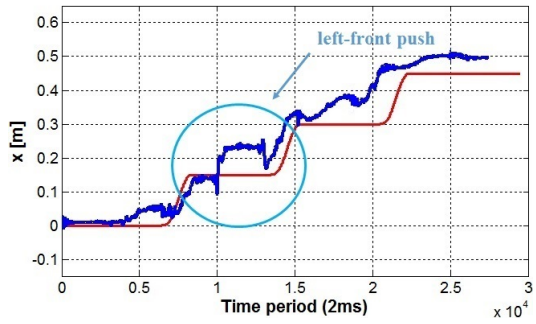

Fig. 6. The X-direction trajectory of the desired ZMP (red line) and the real ZMP (blue line) with push from the left-front.

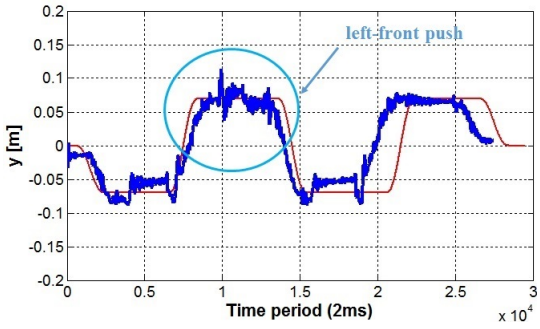

Fig. 7. The Y-direction trajectory of the desired ZMP (red line) and the real ZMP (blue line) with push from the left-front.

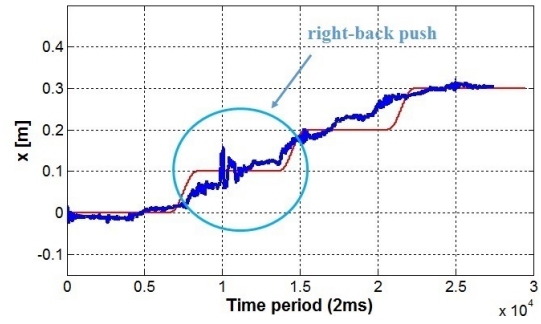

Fig. 8. The X-direction trajectory of the desired ZMP (red line) and the real ZMP (blue line) with push from the right-back.

experiment in X and Y direction are shown in Fig. 6 and Fig. 7. The push comes from the right-back of the robot in the second step. The ZMP trajectory of second experiment in X and Y direction are shown in Fig. 8 and Fig. 9.

VII. CONCLUSIONS AND FUTURE WORK

In this paper, the human-like push-recovery control system is integrated into the general walking pattern generator to react to the perturbations during the walking process. In order to design the human-like motion controller, we analyze the human beings reaction to the external pushes. To reduce the modeling error, the five mass with angular momentum model is implemented to construct the walking pattern generator. Finally, we conduct experiments of different planar directions

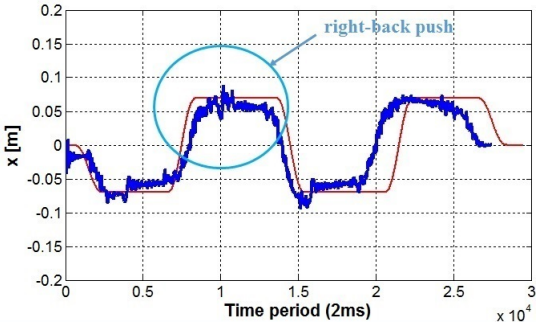

Fig. 9. The Y-direction trajectory of the desired ZMP (red line) and the real ZMP (blue line) with push from the right-back.

pushes on the NTU-iCeiRA humanoid robot and analyze the experimental results to verify the practicability and the feasibilities of the proposed system. In the future, if the strategy based on the capture point theory can be integrated into the push-recovery system, the torque saturation can be largely enhanced.

REFERENCES

[1] M. Vukobratovi and B. Borovac, "Zero-moment pointthirty five years of its life," *International Journal of Humanoid Robotics*, vol. 1, pp.157-173, 2004.

[2] S. Kajita, F. Kanehiro, K. Kaneko, K. Fujiwara, K. Harada, K. Yokoi, et al., "Biped walking pattern generation by using preview control of zero-moment point," in *Robotics and Automation*, 2003. Proceedings. ICRA 03. IEEE International Conference on, 2003, pp. 1620-1626.

[3] S. Shimmyo, T. Sato, and K. Ohnishi, "Biped walking pattern generation by using preview control based on three-mass model," *Industrial Electronics, IEEE Transactions on*, vol. 60, pp. 5137-5147, 2013.

[4] P.-B. Wieber, "Trajectory free linear model predictive control for stable walking in the presence of strong perturbations," in *Humanoid Robots, 2006 6th IEEE-RAS International Conference on*, 2006, pp. 137-142.

[5] J. Pratt, J. Carff, S. Drakunov, and A. Goswami, "Capture point: A step toward humanoid push recovery," in *Humanoid Robots, 2006 6thIEEE-RAS International Conference on*, 2006, pp. 200-207.

[6] Taisuke Kobayashi, Kosuke Sekiyama, Tadayoshi Aoyama, Yasuhisa Hasegawa, and Toshio Fukuda, "Optimal Use of Arm-Swing for Bipedal Walking Control," in *Robotics and Automation (ICRA), 2015 IEEE International Conference on*, 2015, pp. 5698 - 5703.

[7] Albertus Hendrawan Adiwahono, Chee-Meng Chew, Weiwei Huang, and Van Huan Dau, "Humanoid Robot Push Recovery through Walking Phase Modification," in *Robotics Automation and Mechatronics (RAM), 2010 IEEE Conference on*, 2010, pp. 569 - 574.

[8] R. C. Luo, J. Sheng, C.-C. Chen, P.-H. Chang, and C.-I. Lin, "Biped robot push and recovery using flywheel model based walking perturbation counteraction," in *Humanoid Robots (Humanoids), 2013 13th IEEE-RAS International Conference on*, 2013, pp. 50-55.

[9] T. Sato, S. Sakaino, and K.Ohnishi,Real-Time Walking Trajectory Generation Method With Three-Mass Models at Constant Body Height for Three-Dimentional Biped Robots, *IEEE Trans. Ind. Electronics*, vol. 58, no. 2, pp. 376-383, Feb. 2011.

[10] T. Sato, S. Sakaino, and K. Ohnishi, Real-time walking trajectory generation method at constant body height in single support phase for three-dimensional biped robot, in *Proc. IEEE Int. Conf. Technol.*, 2009, pp. 1-6.

[11] R. C. Luo, P. H. Chang, J. Sheng, S. C. Gu, C. H. Chen, Arbitrary biped robot foot gaiting based on variate COM height, in *Proc. IEEE/RAS Int. Conf. Humanoid Robots*, 2013, pp. 534-539.

[12] S. kajita, A. Kobayashi, and T. Yamaura, Dynamic Walking Control of a Biped Robot Along a Potential Conserving Orbit, *IEEE Trans. On Robotics and Automation Society*, vol RA-8, no.4, pp.431-438, 1992.